Multi-wavelength photonic band gaps based on quasi-periodically poled lithium niobate ordered in Fibonacci sequences

Zhuoer Zhou (周琢尔)*, **Jianhong Shi (石剑虹)**, **and Xianfeng Chen (陈险峰)****

Department of Physics, The State Key Laboratory on Fiber-Optic Local Area Network and Advanced Optical Communication Systems, Shanghai Jiao Tong University, Shanghai 200240, China

**E-mail: purewater@sjtu.edu.cn; **e-mail: xfchen@sjtu.edu.cn*

Received September 3, 2008

We demonstrate a quasi-periodic structure exhibiting multiple photonic band gaps (PBGs) based on sub-micron-period poled lithium niobate (LN). The structure consists of two building blocks, each containing a pair of antiparallel poled domains, arranged as a Fibonacci sequence. The gap wavelengths are analyzed with the Fibonacci sequence parameters such as the quasiperiodic indices and the average lattice parameter. The transmission properties are investigated by a traditional 4×4 matrix method. It has also been proved that the gap depth can be tuned by the lengths of poled domains.

OCIS codes: 160.3730, 230.5298.

doi: 10.3788/COL20090706.0508.

Photonic crystals (PCs) are a class of dielectric materials artificially fabricated with periodicity. With a proper design, these structures could exhibit the essential properties of forbidden frequency bands from which propagating modes are absent[1−3]. There has been great interest in photonic band gap (PBG) structures for potential applications in light flow manipulations also.

Nonlinear photonic crystals (NPCs) are nonlinear crystals with some parts of inversed polarization directions. The positive domain and negative one are periodically layered, so the nonlinear coefficient $\chi^{(2)}$ is periodically changed with the signs in space but keeps its magnitude constant[4]. The NPCs can be fabricated by periodically poling ferroelectric materials such as lithium niobate (LN) and $KTiOPO_4$ (KTP), expected to be useful in the quasi phase matching (QPM) technique[5−8].

With the maturity and advanced exploration in ferroelectrics domain engineering, there have been more attempts in acquiring much thinner domain shapes. It has been reported recently that the scale of domain thickness of such ferroelectrics as KTP isomorphs and $LiNbO_3$ has been improved to the level of sub-microns[8−13]. The deceasing of domain structure has caught lots of interests for its promising applications, for example the realization mirrorless optical parametric oscillators (OPOs) for coherent and tunable light sources demonstrated in sub-micron periodically poled KTP[14]. Based on a single chip of sub-micron periodically poled lithium niobate (PPLN), we have proposed a narrow PBG structure which is generated by Bragg scattering[15]. The formation of the gap is due to the contra-directional coupling between two orthogonally polarized states caused by the azimuth angle perturbations between the principal axes.

Besides the studies on periodic multilayers, many efforts have been devoted to the applications on quasi-periodic structures which have given rise to some interesting phenomena not observed in periodic structures. For example, a strong suppression of the optical transmission in quasi-periodic dielectric multilayer stacks of SiO_2 and TiO_2 thin films has been observed[16]. In the case of a $\chi^{(2)}$ nonlinear quasi-periodic PC, high efficient QPM third harmonic generation in a quasi-periodic optical superlattice of $LiTaO_3$ was reported and the generation of coherent terahertz radiation with multi-frequency modes in a quasi-periodically poled lithium niobate (QPLN) with a Fibonacci sequence was also proposed theoretically[17,18].

In this letter, we report that a sub-micron QPLN (SQPLN) ordered in Fibonacci sequence can demonstrate multiple PBGs. The basic building blocks A and B are supposed to be of sub-micron level thickness. The central wavelengths of gaps are analyzed by the indices concerning the quasi-periodicity of a Fibonacci sequence and the average lattice parameter. The transmittances of the gaps with different indices can be tuned by varying structure parameters such as the lengths of poled domains.

Figure 1 shows the schematic of experimental setup for a SQPLN multi-PBG structure. We consider the case of normally incident plane waves. Previously we have discussed that PPLN would act as a Solc filter when the

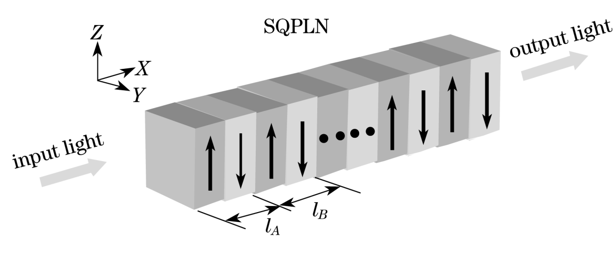

Fig. 1. Schematic of experimental setup for a SQPLN multi-PBG structure. The plane waves are normally incident. The arrows indicate the polarization direction of each domain. X, Y, and Z represent the principal axes of the original index ellipsoid of $LiNbO_3$. l_A and l_B represent the lengths of two building blocks A and B, respectively.

principal axis of each domain has a rotation angle compared with the original one as each of the domain is a half-wave plate[19]. The domain period is supposed to be tens of microns in such applications. While the domain length of such a periodical structure decreases down to microns or sub-microns, which is comparable to the wavelength of the input light, the alternated positive and negative rotation angles will induce contra-directional coupling between two orthogonally polarized modes, and forbidden band gaps can occur in such media when the following Bragg condition is satisfied:

$$(k_1^+ + k_2^+)\cdot\kappa + (k_1^- + k_2^-)\cdot(1-\kappa) - \frac{m\pi}{\Lambda} = 0, \quad m = 1,2,3,\cdots, \qquad (1)$$

where $k_1^{\pm}$ and $k_2^{\pm}$ are the wave-vectors defined by $\frac{2\pi n_e^{\pm}}{\lambda}$ and $\frac{2\pi n_o^{\pm}}{\lambda}$, and the scripts '+' and '−' indicate the positive domain and negative domain, n_e and n_o are the extraordinary and ordinary indices, respectively; κ is the proportional number of positive domain length to the period length and $0 < \kappa < 1$; m is the coupling order and Λ is the period of PPLN which is the sum length of one positive domain and one negative domain.

For the case $\kappa = 0.5$, Eq. (1) can be rewritten in a more simplified wavelength expression form as

$$\lambda_m = \frac{1}{2m+1}(n_o + n_e)\Lambda. \qquad (2)$$

The building blocks are ordered in a Fibonacci sequence according to the production rule $F_i = F_{i-1}|F_{i-2}$ for $i \geq 3$, with $F_1=\{A\}$ and $F_2=\{AB\}$. Each block has a domain of length $l_{A1}l_{B1}$ with positive ferroelectric domain and a domain of length $l_{A2}l_{B2}$ with negative ferroelectric domain.

The formula of gap wavelength can be extended from a periodic structure to a quasi-periodic structure. The wavelengths of SQPLN mulit-PBGs with a Fibonacci sequence are given by

$$\lambda_{p,q} = (n_o + n_e)\Lambda_{p,q}, \qquad (3)$$

where m equals zero in this application; $\Lambda_{p,q} = L/(p + q\tau)$, p and q are integer indices of the quasi-periodicity, $\tau = (1+\sqrt{5})/2$ which is so-called the golden ratio, and $L = \tau l_A + l_B$ is the average lattice parameter[18,20]. Furthermore, the structural parameter l can also be adjusted in our simulations.

The transmission spectrum can be simulated by the 4×4 transfer matrix[21−23] considering that the electromagnetic wave is composed of four partial waves traveling in such a birefringent medium. The transfer matrix of a single domain is the production of two component matrices D and P. The matrix D is given by

$$D(\theta) = \begin{pmatrix} \cos\theta & \cos\theta & -\sin\theta & -\sin\theta \\ n_o\cos\theta & -n_o\cos\theta & -n_e\sin\theta & n_e\sin\theta \\ \sin\theta & \sin\theta & \cos\theta & \cos\theta \\ -n_o\sin\theta & n_o\sin\theta & -n_e\cos\theta & n_e\cos\theta \end{pmatrix}, \qquad (4)$$

and the matrix P is given by

$$P(x) = \begin{pmatrix} \exp(-i\pi n_o x/\lambda) & 0 & 0 & 0 \\ 0 & \exp(i\pi n_o x/\lambda) & 0 & 0 \\ 0 & 0 & \exp(-i\pi n_e x/\lambda) & 0 \\ 0 & 0 & 0 & \exp(i\pi n_e x/\lambda) \end{pmatrix}, \qquad (5)$$

where θ is an azimuth angle between Z axis and Y axis; x is the thickness of a domain. By multiplication for N domains, we get the general form of total transfer matrix as

$$M = D_a^{-1}[D(-\theta)P(b)D^{-1}(-\theta) \times D(\theta)P(a)D(\theta)]^N D_a, \qquad (6)$$

where D_a is the dynamic matrix of air given by

$$D_a = \begin{pmatrix} 1 & 1 & 0 & 0 \\ 1 & -1 & 0 & 0 \\ 0 & 0 & 1 & 1 \\ 0 & 0 & -1 & 1 \end{pmatrix},$$

a is the length of positive domain, and b is the length of negative domain.

In case of normally incident plane waves, the specific transmission or reflection coefficients could be derived from M. For example, the transmission of Y direction output with the same direction input is expressed as

$$T_{yy} = \left| \frac{M(1,1)}{M(1,1)M(3,3) - M(1,3)M(3,1)} \right|^2. \qquad (7)$$

As the propagation behaviors and transmission properties of T_{yy} are similar to T_{zz} (Z-output with Z-input case), we only discuss the Y direction case for simplicity throughout the letter.

Figure 2 shows the transmission spectrum of the SQPLN multi-PBG structure consisting of 17711 building blocks of A and 10946 building blocks of B, which are arranged in order of the sequence of $F21$, in the wavelength range from 950 to 1600 nm. $l_A = 421$ nm, $l_B = 260$ nm, and $l_{A2} = l_{B2} = l = 200$ nm. n_e and n_o are chosen to be 2.1381 and 2.2112, respectively. The azimuth angle θ is set to be $\pi/1000$ and the polarization of the incident light is along Y-direction throughout the simulations. The quasi-periodic indices corresponding to the band gap wavelengths are given in the figure. At the main or so-called central frequency of principal gap wavelength corresponding to the quasi-periodic index (1,1), the width of the gap defined by the wavelength where the transmission is lower than 1% is 0.123 nm. In Table 1, we compare the wavelengths of gap obtained from simulations and the theoretical ones from Eq. (3). The simulated gap wavelengths match well with the theoretical ones.

Besides the most intense gap taken with a quasi-periodical index (1,1), some other gap modes, labeled by (1,2), (0,2), and so on did not show deep gaps with the parameters given in Fig. 2. The transmittance at $\lambda_{1,2}$ is about 8% and the transmittance at $\lambda_{0,2}$ is about 32%.

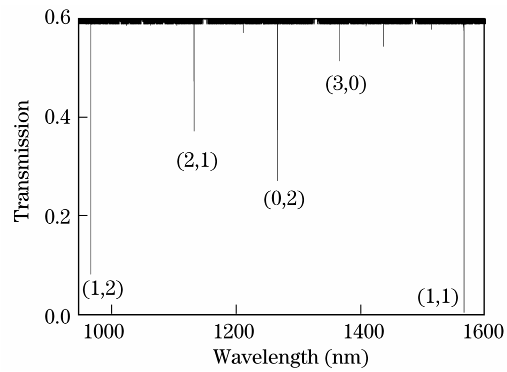

Fig. 2. Transmission spectrum of a SQPLN multi-PBG structure in the wavelength range of 950 − 1600 nm. The structure consists of 17711 building blocks of A and 10946 building blocks of B, which are arranged in order of the sequence of $F21$. $l_A = 421$ nm, $l_B = 260$ nm, $l_{A2} = l_{B2} = l = 200$ nm, $n_e = 2.1381$, $n_o = 2.2112$.

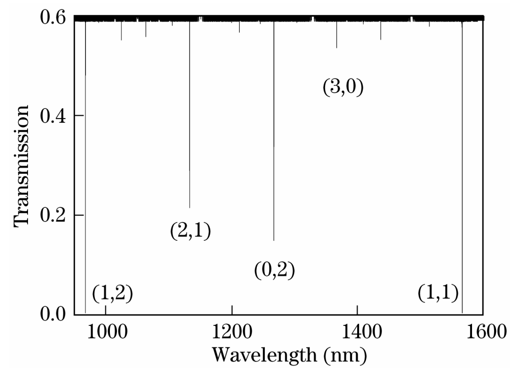

Fig. 3. Transmission spectrum of a SQPLN multi-PBG structure in the wavelength range of 950 − 1600 nm. The structure consists of 17711 building blocks of A and 10946 building blocks of B, which are arranged in order of the sequence of $F21$. $l_A = 421$ nm, $l_B = 260$ nm, $l_{A2} = l_{B2} = l$ =130 nm, n_e = 2.1381, $n_o = 2.2112$.

Table 1. Quasi-Periodic Indices and Band Gap Wavelengths

p, q	1,0	0,1	2,0	1,1	3,0
Theoretical					
$\lambda_{p,q}$ (nm)	4099.3	2533.5	2049.6	1565.8	1366.4
Simulated					
$\lambda_{p,q}$ (nm)	···	···	···	1565.8	1366.4
p, q	0,2	2,1	1,2	0,3	
Theoretical					
$\lambda_{p,q}$ (nm)	1266.8	1133	967.72	844.5	
Simulated					
$\lambda_{p,q}$ (nm)	1266.76	1133.02	967.72	···	

Table 2. Fourier Amplitude Component $d_{p,q}/d_0$ for the Quasi-Periodic Indices Corresponding to the Observed Gap Wavelengths

p, q	1,1	3,0	0,2	2,1	1,2
$\lambda_{p,q}$	(1565.8)	(1366.4)	(1266.8)	(1133.0)	(967.72)
$d_{p,q}/d_0$	0.3924	0.0401	0.0834	0.0487	0.0969

$l_A = 421$ nm, $l_B = 260$ nm, $l_{A2} = l_{B2} = l = 200$ nm, and $\tau = (1+\sqrt{5})/2$.

Meanwhile, the gap shape is not clearly observed at $\lambda_{3,0}$.

The wavelength-dependent gap depth can be sought from the Fourier amplitude component of a Fibonacci sequence $d_{p,q}$ for the gap wavelength given by

$$d_{p,q} = d_0 \sin(X_{p,q}) \sin(\pi l/\Lambda_{p,q})/(X_{p,q}\pi l/\Lambda_{p,q}), \qquad (8)$$

where d_0 is a constant and $X_{p,q} = \pi\tau^2(pl_A - ql_B)/L$. We calculated the magnitude of $d_{p,q}/d_0$ for $(p, q) = (1,1), (3,0), (0,2), (2,1), (1,2)$. The results are shown in Table 2. It is worth noting that the transmittances of the SQPLN gap can be changed by varying the poled domain length such as the length of the negative poled domain. Figure 3 shows the transmission spectrum of the multi-PBG structure on SQPLN in the wavelength range of 950 − 1600 nm when $l_A = 421$ nm, $l_B = 260$ nm, and $l_{A2} = l_{B2} = l = 130$ nm. One can see that the transmittance at $\lambda_{1,2}$ of 967.72 nm significantly decreases and the full gap shape forms at the corresponding location. The widths of gaps at $\lambda_{1,1}$ and $\lambda_{1,2}$ are 0.107 and 0.066 nm, respectively.

We have systematically investigated the transmittances of the SQPLN gaps by varying the negative domains of building block A (l_{A2}) and building block B (l_{B2}). In simulations, l_{A2} and l_{B2} were assumed to be the same, that is, $l_{A2} = l_{B2} = l$ and the total domain lengths of building block A (l_A) and building block B (l_B) were kept to be 421 nm and 260 nm, respectively. This structure is of benefit to fabricate because it is easy to pole the same size domains in the electric poling technique. Figure 4 shows the dependence of the transmittances at $\lambda_{1,1}$, $\lambda_{1,2}$, $\lambda_{2,1}$, and $\lambda_{0,2}$ on l that changes from 0 to 260 nm. The transmittances at $\lambda_{1,1}$ and $\lambda_{1,2}$ are below 0.5% and deep non-transmitted frequency gaps are formed when l is in the range from 120 to 170 nm.

For the case of $l = 223$ nm, the transmittance at $\lambda_{1,1}$ is below 0.3%, while the transmittance at $\lambda_{1,2}$ is approaching to 60%. It is noted that the transmittance curve shows a turning point at 223 nm where occurs to be the zero-order QPM length for $\lambda_{1,2}$. The characteristics of the transmittances at other gap wavelengths of $\lambda_{2,1}$ and $\lambda_{0,2}$ are similar to those of $\lambda_{1,2}$. However,

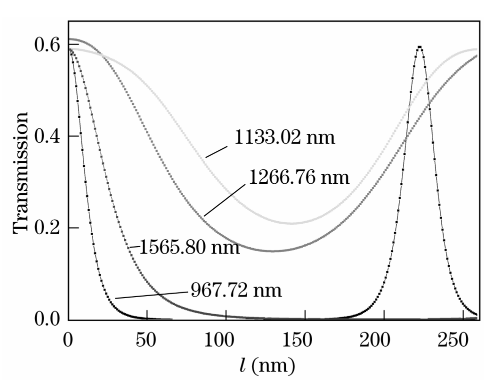

Fig. 4. Dependence of transmittances at $\lambda_{1,1}$, $\lambda_{1,2}$, $\lambda_{2,1}$, and $\lambda_{0,2}$ on the uniform length of negative domain l that changes from 0 to 260 nm. In simulations, $l_{A2} = l_{B2} = l$ and the total domain lengths of building block A (l_A) and building block B (l_B) are kept to be 421 and 260 nm, respectively.

they could not touch the very low gap with their lowest transmittances around 14% and 21%. The fact that the gap depth can be tuned by varying the negative domain length is very useful in implementing the SQPLN multi-PBG structures. Practically, because the poling procedure of the same size in building blocks of A and B has been simplified in a conventional poling technique, the needed gaps could be designed by setting a proper negative domain length at the same time.

In conclusion, we show that a $\chi^{(2)}$ nonlinear quasi-periodic PC crystal with a Fibonacci sequence can act as a multi-PBG structure. The simulated gap wavelengths match well with the theoretical results expressed by quasi-periodic integer indices and the average lattice parameter. The gap depth can be tuned by varying the structural parameters such as the lengths of the negative or positive domains. The multiple narrow band gaps would be promising in controlling the light behavior and lead to a number of useful applications.

This work was supported by the National Natural Science Foundation of China (Nos. 60508015 and 10876019), the National "973" Program of China (No. 2007CB307000), the Shanghai Education Development Foundation (No. 2007CG015), and the Shanghai Leading Academic Discipline Project (B201).

References

1. E. Yablonovitch, Phys. Rev. Lett. **58,** 2059 (1987).
2. S. John, Phys. Rev. Lett. **58,** 2486 (1987).
3. E. Yablonovitch, T. J. Gmitter, and K. M. Leung, Phys. Rev. Lett. **67,** 2295 (1991).
4. V. Berger, Phys. Rev. Lett. **81,** 4136 (1998).
5. R. L. Byer, J. Nonlin. Opt. Phys. Mater. **6,** 549 (1997).
6. L. E. Myers, R. C. Eckardt, M. M. Fejer, R. L. Byer, W. R. Bosenberg, and J. W. Pierce, J. Opt. Soc. Am. B **12,** 2102 (1995).
7. K. Mizuuchi and K. Yamamoto, Opt. Lett. **23,** 1880 (1998).
8. M. Yamada, N. Nada, M. Saitoh, and K. Watanabe, Appl. Phys. Lett. **62,** 435 (1993).
9. C. Canalias, V. Pasiskevicius, R. Clemens, and F. Laurell, Appl. Phys. Lett. **82,** 4233 (2003).
10. V. Dierolf and C. Sandmann, Appl. Phys. Lett. **84,** 3987 (2004).
11. M. Müller, E. Soergel, and K. Buse, Appl. Phys. Lett. **83,** 1824 (2003).
12. M. Fujimura, T. Sohmura, and T. Suhara, Electron. Lett. **39,** 719 (2003).
13. Y. Zhi, D. Liu, W. Qu, Y. Zhou, L. Liu, and Y. Hang, Acta Opt. Sin. (in Chinese) **27,** 2220 (2007).
14. C. Canalias and V. Pasiskevicius, Nature Photon. **1,** 459 (2007).
15. Z. Zhou, J. Shi, and X. Chen, "Electrical induced and tunable photonic band gap in submicron periodically poled lithium niobate" submitted to Appl. Phys. B.
16. W. Gellermann, M. Kohmoto, B. Sutherland, and P. C. Taylor, Phys. Rev. Lett. **72,** 633 (1994).
17. S. Zhu, Y. Zhu, and N. Ming, Science **278,** 843 (1997).
18. Y. Qin, H. Su, and S. Tang, Appl. Phys. Lett. **83,** 1071 (2003).
19. X. Chen, J. Shi, Y. Chen, Y. Zhu, Y. Xia, and Y. Chen, Opt. Lett. **28,** 2115 (2003).
20. Y. Zhu and N. Ming, Phys. Rev. B **42,** 3676 (1990).
21. P. Yeh, *Optical Waves in Layered Media* (Wiley, New York, 1988).
22. P. Yeh, J. Opt. Soc. Am. **69,** 742 (1979).
23. A. Mandatori, C. Sibilia, M. Centini, G. D'Aguanno, M. Bertolotti, M. Scalora, M. Bloemer, and C. M. Bowden, J. Opt. Soc. Am. B **20,** 504 (2003)